Turbulent Convective Heat and Mass Transfer From Accelerating Particles

I. S. PASTERNAK and W. H. GAUVIN

McGill University, Montreal, Quebec, Canada

The rate of evaporation of acetone from single particles accelerating freely in a downward concurrent turbulent air stream was studied over a range of air velocities from 40 to 70 ft./sec. and at a constant air temperature of 410°F. The particles consisted of celite in the shape of spheres, cubes, disks and cylinders, varying in size from 0.15 to 0.40 in. Accurate particle velocity data were obtained with a new radioactive tracer technique, and high-speed photography at two positions along the column permitted measurement of the rate of rotation and showed that the particles rotated in a random manner.

Adequate prediction of the observed heat and mass transfer data could be obtained from the integration of a rate equation previously reported for stationary particles. The concept of a new characteristic dimension, developed for the latter case, was found to be applicable to randomly rotating shapes and to account satisfactorily for the behaviour of nonspherical particles.

Information on the rates of heat and mass transfer from particles in a fluid stream is necessary in such engineering applications as flash drying and most solids-gas contacting operations. A knowledge of such data is indispensable for design calculations, and their correlation is of considerable importance in the theoretical development of particulate systems.

A previous study (*1*) has shown that for a stationary particle of a given shape suspended in a fluid stream in a definite orientation the convective mass transfer rate is given by

$$j_D = 0.692(N_{Re}'')^{-0.488} \text{ for } 500 < N_{Re}'' < 5{,}000 \quad (1)$$

This expression was obtained for an intensity of turbulence of the fluid stream of 10%. If the value of the log mean pressure of the air in the particle boundary layer is close to the total pressure, Equation (1) can be put in the equivalent form:

$$N_{Nu'} = 0.692\ (N_{Re}'')^{0.514}\ (N_{Sc})^{1/3} \quad (2)$$

In both expressions N_{Re}'' and $N_{Nu'}$ are based on a new particle characteristic dimension L'' (defined as the total surface area of the particle divided by the perimeter of the maximum projected area perpendicular to flow) which is believed to account for the average thickness of the boundary layer for heat and mass transfer.

Equation (1) permitted the correlation of all the experimental data on twenty shapes in different orientations with a maximum deviation of ± 15%, as well as that of many published results in the literature.

It can be predicted that in the case of a particle freely accelerating and rotating in a hot turbulent air stream the rate of heat and mass transfer will be affected to a slight extent by the acceleration (*2*) and by the rotation of the particle (*3*), and probably to a larger extent by the relative intensity of turbulence of the air stream (*4*) as well as the high evaporation rate from the particle (*5, 6*). Finally there still remains the problem of accounting for the influence of the particle shape on the transfer phenomena.

Some data are available in the literature on the rates of heat and mass transfer from accelerating and decelerating droplets and spheres in turbulent air streams (*7, 8*), but little information could be found for other shapes owing partly to the lack of a well-defined characteristic dimension for a rotating shape and partly to the inadequacy of existing correlations or experimental methods to describe accurately the velocity of a particle accelerating in a turbulent air stream.

The present investigation was undertaken to obtain turbulent heat and mass data for freely accelerating, rotating particles at various concurrent air velocities and to extend the definition of the characteristic dimension to randomly rotating particles so that it may be used in heat and mass transfer correlations.

EXPERIMENTAL

The rate of evaporation of acetone from particles accelerating concurrently in a hot turbulent air stream was studied in a 17.64 ft. long, 1½-in. diameter Pyrex glass column.

Particle Shapes

All the particles used were accurately made from celite because of the strength, porosity, inertness, and workability of this material. The particular shapes studied were spheres, cubes, and cylinders. Table

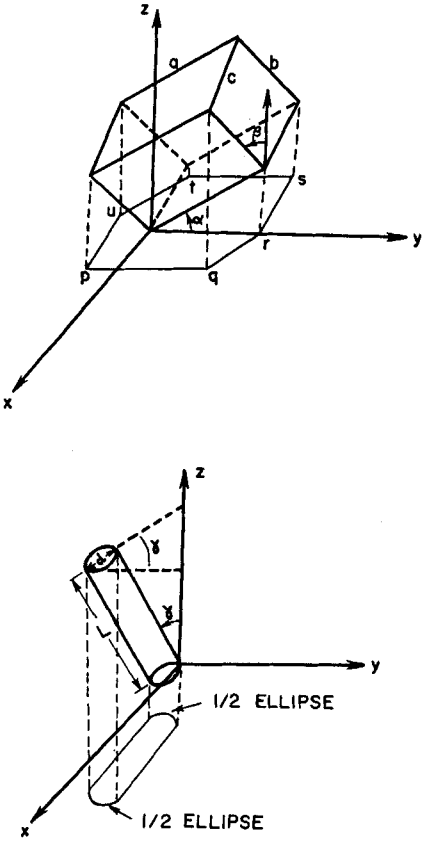

Fig. 1. Rotating prism and cylinder.

I. S. Pasternak is presently with Imperial Oil Limited, Sarnia, Ontario, Canada.

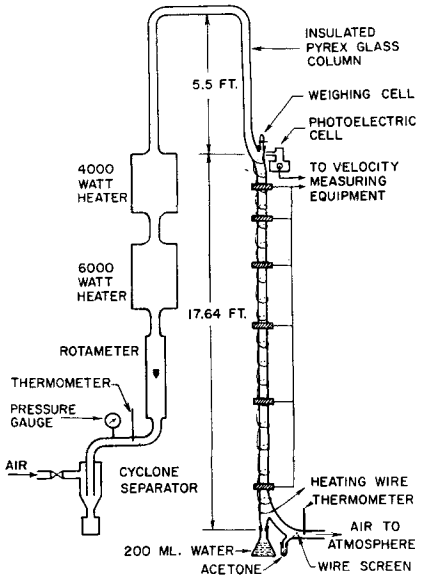

Fig. 2. Schematic diagram of apparatus.

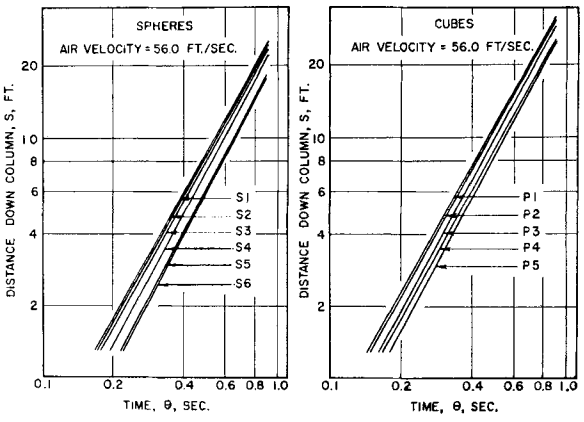

Fig. 3. Distance-time graphs for spheres and cubes.

1 shows the dimensions of these shapes together with λ, an average calculated value of L'', evaluated over all possible random orientations. Thus for a freely rotating particle the characteristic dimension λ is now defined as the ratio of the total surface area of the particle to the average value of the perimeter of the projected area perpendicular to flow. To evaluate the latter, two cases will be considered: the rotating prism and the rotating cylinder. (For a sphere, obviously, $L'' = \lambda = D$.)

The Rotating Prism—Consider a prism with sides a, b, and c units long and assume that the prism rotates freely in a xyz co-ordinate system favoring no particular orientation. Figure 1 shows the prism momentarily in a position such that it has rotated through an angle α in the y-plane and through an angle β in the x-plane. If the air flow is in the z-direction, then the average perimeter of the required shadow ($pqrstu$), in a plane perpendicular to the z-axis, can be found by considering the rotation of the prism simultaneously about the x and y axes; thus average projected

$$\text{perimeter} = (2)/(\pi/2)\int_0^{\pi/2} a\cos\alpha\, d\alpha + (2)(b+c)/(\pi^2/4)\int_0^{\pi/2}\int_0^{\pi/2}\sqrt{1-\sin^2\beta\sin^2\alpha}\, d\beta d\alpha \quad (3)$$

$$= 1.27\,a + 1.72\,(b+c) \quad (4)$$

Putting this equation in a form symmetrical in a, b, and c one obtains average

$$\text{perimeter} = 1.57\,(a+b+c) \quad (5)$$

$$\text{Hence } \lambda = \frac{\text{total surface area}}{\text{average perimeter}} = 1.27\,\frac{(ab+bc+ac)}{(a+b+c)} \quad (6)$$

For the special case of a cube with side a units

$$\lambda = 1.27\,a \quad (7)$$

The Rotating Cylinder—Consider a cylinder of length L units and diameter d units and again assume that the cylinder will rotate freely in a xyz co-ordinate system favoring no particular orientation. Figure 1 shows the cylinder in a position such that it makes an angle γ in the x-plane. As before average projected perimeter

$$= \frac{2}{\pi}\int_0^{\pi/2}\left[2\,L\sin\gamma + \pi d\sqrt{\frac{1+\cos^2\gamma}{2}}\right]d\gamma \quad (8)$$

$$= 1.27\,(L + 2.12\,d) \quad (9)$$

$$\text{Hence } \lambda = \frac{\text{total surface area}}{\text{average perimeter}} = 2.47\,d\left[\frac{L+(1/2)d}{L+2.12\,d}\right] \quad (10)$$

TABLE 1. PARTICLE SHAPES AND DIMENSIONS

Particle	Designation	Diameter, in.	Length, in.	D_p, in.	λ, in.	Results
Spheres	S1	0.194		0.194	0.194	Figure 4
	S2	0.249		0.249	0.249	
	S3	0.294		0.294	0.294	
	S4	0.320		0.320	0.320	
	S5	0.361		0.361	0.361	
	S6	0.388		0.388	0.388	
Cubes	P1		0.157	0.195	0.199	Figure 5
	P2		0.202	0.250	0.256	
	P3		0.238	0.295	0.302	
	P4		0.260	0.322	0.330	
	P5		0.292	0.362	0.371	
	P6		0.125	0.155	0.159	
	P7		0.150	0.186	0.190	
	P8		0.170	0.211	0.216	
	P9		0.225	0.279	0.286	
	P10		0.251	0.311	0.319	
	P11		0.275	0.341	0.350	
Cylinders	C1	0.169	0.150	0.186	0.193	Figure 6
	C2	0.169	0.201	0.205	0.214	
	C3	0.170	0.251	0.222	0.231	
	C4	0.172	0.298	0.237	0.246	
	C5	0.261	0.101	0.218	0.228	
	C6	0.260	0.150	0.248	0.256	
	C7	0.264	0.200	0.276	0.285	
	C8	0.262	0.251	0.296	0.307	
	C9	0.265	0.300	0.316	0.330	
	C10	0.326	0.198	0.316	0.327	
	C11	0.325	0.300	0.362	0.376	

Evaporating Liquid

Since acetone is both highly volatile and readily determined by analysis in aqueous solutions, it was selected to impregnate the celite particles under study. Acetone reacts quantitatively with iodine in aqueous potassium hydroxide to form a precipitate of iodoform (*9, 10*), in accordance with

$$CH_3COCH_3 + 3I_2 + 4KOH \rightleftarrows CHI_3 + CH_3COOK + 3KI + 3H_2O \quad (11)$$

The amount of excess iodine can be determined by a back titration with sodium thiosulphate as follows:

$$2Na_2S_2O_3 + I_2\ (\text{excess}) \xrightarrow[\text{HCl solution}]{\text{starch}} Na_2S_4O_6 + 2NaI \quad (12)$$

From these two reactions it was possible to analyze for one part of acetone by

weight in 10,000 parts of water with an error of approximately 1%.

Velocity Measuring Technique

A detailed description of the new velocity measuring technique developed by the authors in collaboration with other workers to determine the velocity history of a radioactive particle moving in a fluid stream has been published elsewhere (*11*). In the present application it was found that celite became sufficiently radioactive in a 72-hr. irradiation period in the Chalk River N.R.X. reactor, at a flux density of 8.6 x 10^{12} neutrons/(sq. cm.)(sec.), so that it could be used with the new technique for five days. During a particular experimental run the individual acetone-impregnated, radioactive celite particles were tracked by Geiger probes placed at definite accurately known intervals along the outside surface of the insulated glass column. Sharp timing pulses on the screen of a cathode ray oscilloscope (connected to the output of the probes) were obtained as each probe was activated by a moving particle. A pulse generator, used to calibrate the sweep time of the oscilloscope, enabled the interval between pulses to be obtained to the nearest 1/1,000 sec. A very sensitive photoelectric cell supplied by a 300-v. power pack triggered the oscilloscope when a particle was released into the air stream. A camera equipped with a 5.0-cm. lens was used to photograph the oscilloscope traces. The time between peaks on these traces, corresponding to fixed probe positions along the column, was then read on a projecting microscope equipped with a calibrated stage.

Apparatus

As shown in Figure 2 the apparatus consisted essentially of a 17.64 ft. long, 1½-in. diameter, magnesia-insulated, Pyrex glass test section, preceded by a 5½ ft. length of same diameter to allow the establishment of a fully developed turbulent flow. A smooth S-bend between the two sections facilitated the introduction of the particle under test.

Air supplied by a compressor was passed in succession through a cyclone separator, a calibrated rotameter, two electrical heaters (6,000 w. and 4,000 w., respectively) and finally down the Pyrex glass column. An indicating temperature controller regulated the electrical input to the 6,000-w. heater, while the 4,000-w. heater was kept active continuously. A variac-controlled current through a resistance wire coiled around the column test section (under the magnesia insulation) ensured that the air temperature along the length of the column remained constant. A wire screen at the air outlet from the column was used to prevent any uncollected radioactive particles from leaving the equipment.

Procedure

All experimental runs were carried out at a constant air temperature of 410°F. After steady conditions of air velocity and temperature had been obtained in the column, an acetone-impregnated, radioactive celite particle of known dry weight was placed in an air-tight teflon and aluminum weighing cell and the acetone content in the particle determined on an analytical balance. In all cases the amount of acetone was more than sufficient to insure evaporation under free liquid surface conditions throughout the column. The cell containing the particle was then placed for 5 to 10 min. in a water bath preset at a temperature corresponding to the acetone wet-bulb temperature of the hot air (19.7°C.) which was experimentally determined and not calculated from simple wet-bulb theory. The particle was thus introduced into the air stream under equilibrium conditions. It is important to note that in all cases the water wet-bulb temperature of the air was in the range 14° to 15°C., thus eliminating the possibility of water vapor being transferred to the acetone on the particle. Had the acetone temperature been below the water wet-bulb volume, such reverse mass transfer would have occurred, which would have undoubtedly influenced the evaporation of acetone.

Meanwhile the velocity-measuring equipment was activated and the camera shutter was opened to record the cathode-ray oscilloscope trace. The particle in the cell was then placed over the test section (at the S-bend), the cell opened (by a sliding gate), and the particle released into the flowing air stream. At this moment the photoelectric cell, activated by the passing particle, triggered the oscilloscope, and a permanent record of the sharp pulses from the probes was obtained on the film. The sweep time of the oscilloscope was always made greater than the residence time of a particular particle in the column.

On reaching the end of the column, the particle fell into a flask containing exactly 200 ml. of cold distilled water. In this way acetone evaporation was instantly stopped. To determine the acetone content left in the particle the solution in the flask containing the particle was boiled under reflux for 10 min. to allow acetone to diffuse from the particle into the water. An aliquot of the water-acetone solution was then withdrawn with a pipette and the amount of acetone determined by the iodine-sodium thiosulphate titration previously described. The precision of the analytical method was checked with blank runs carried out on celite spheres impregnated with known amounts of acetone. The results indicated that an average of 1.29% of the initial acetone content appeared to remain in a particle at the end of 10 min. of boiling under reflux. All subsequent results were therefore corrected for this deviation.

Table 2. Particle Rotation Data

Position in column	Particle no.	Air velocity, ft./sec.	Manner and speed of rotation, (r.p.s. = rotations per second)
Top	S4	40.0	30 r.p.s. in both directions perpendicular to flow; 42 r.p.s. parallel to flow direction.
Top	S4	62.1	15 r.p.s. in one direction perpendicular to flow; 30 r.p.s. parallel to flow direction.
Bottom	P3	62.1	90 r.p.s. completely random rotation.
Bottom	C9	62.1	22 r.p.s. around an axis perpendicular to the length of the cylinder.
Bottom	C10	62.1	88 r.p.s. around an axis perpendicular to the length of the cylinder.

EXPERIMENTAL RESULTS

Ninety-six experimental runs were carried out with spheres, cubes, and cylinders with air velocities from 40.0 to 70.0 ft./sec. at a constant temperature of 410°F.*

Velocity Data

Figure 3 shows typical distance-time graphs obtained by the radioactive tracer technique. It was found that the data for all shapes fell along straight lines when plotted on log-log graph paper. This allowed a distance-time equation to be obtained for each run from which, by differentiation, the instantaneous absolute velocity and acceleration as well as the relative velocity and the Reynolds number of a particle could be determined at any point down the column. The reproducibility of the velocity data for all shapes was good, and in all cases the velocity of the particle was always less than that of the air.

Values of the coefficient of drag were calculated as a function of the Reynolds number for each of the spheres and other particles. They are not shown here because of the uncertainty of the particle path. If the average air velocity is used in the calculation of the particle relative velocity, these values are invariably larger

* Tables of data and results have been deposited as document No. 6619 with the American Documentation Institute, Photoduplication Service, Library of Congress, Washington 25, D. C., and may be obtained for $1.25 for photoprints and for 35-mm. microfilm.

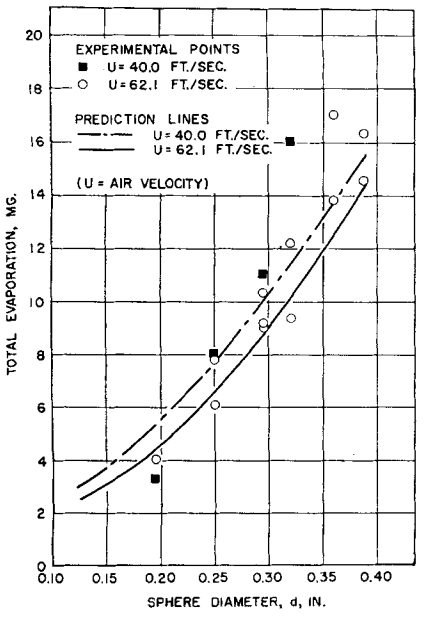

Fig. 4. Total evaporation for a sphere as a function of its diameter and the air velocity.

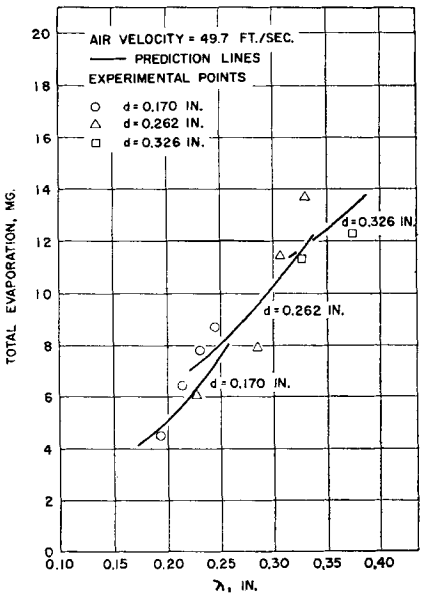

Fig. 5. Total evaporation for a cube as a function of its characteristic dimension and the air velocity.

than those given by the standard curves of C_D vs. Re of Lapple and Shepherd (*12*) and show a strong dependency on the diameter or λ of the particle. If the maximum air velocity is used, the coefficients of drag form a family of curves, with the particle diameter as parameter, each curve dipping sharply to a minimum value below the standard curve. These curves bear much resemblance to those obtained by Torobin (*13*), using the relative intensity of turbulence as parameter, the latter being defined as the ratio of the root-mean-square value of the velocity fluctuations in the axial direction to the particle relative velocity. Torobin has shown that for spheres at low relative intensities the drag coefficients do not differ appreciably from the standard values reported for laminar fluids. As the relative intensities increase, there is a gradual and moderate increase in the momentum transfer, during which turbulence affects the vorticity transfer in the wake alone. A further intensity increase causes the drag coefficient vs. Reynolds number curve to drop gradually at first and then sharply to a minimum, owing to a laminar-turbulent transition in the attached boundary layer in a manner analogous to the well-known behavior at N_{Re} of 250,000 to 300,000 in laminar fluids. He also showed that the product of the square of the relative intensity of turbulence and of the critical value of the Reynolds number at which transition occurred was a constant, with a value of 45 for his system, and that the phenomenon was not affected by acceleration. The important conclusion, as far as the present study is concerned, that can be drawn from Torobin's work is that some of the particles tested, particularly the larger ones, must have undergone transition, since the relative intensity of turbulence increased from an approximate value of 3% at the top of the column, with fully developed turbulent air flow (*14*) assumed, to an approximate value of 25% at the bottom.

The motion of a few of the particles was photographed with a high-speed 16-mm. cine-camera operated at 5,000 frames/sec. It was observed that the S-bend of the column, at the point of introduction of a particle, did not cause the particles to deviate from the center of the column and in almost all cases they appeared to travel along the axis. However when a particle did hit the walls of the column, it did so in a glancing manner with little apparent effect on the particle velocity.

Table 2 summarizes some of the observations. The actual films have been shown elsewhere (*15*). The high-speed photographs clearly showed that in all cases random rotation of a particle occurred as it travelled down the column, thus justifying the use of the average dimension λ to characterize the particle.

Mass Transfer Data

Each of the ninety-six runs yielded the amount of acetone evaporated by each particle under a given set of conditions as the direct experimental result. It might appear, at first sight, that this information could have been correlated and plotted in a number of conventional ways. It must be appreciated, however, that since the rate of mass transfer is a function of the particle Reynolds number, the rate of evaporation will continuously decrease as the particle accelerates down the column or, in other words, as its relative velocity decreases. Although the instantaneous values of the Reynolds number are known (from Figure 3), the corresponding instantaneous quasi-steady state values of the evaporation rate are not. Only the total amount of evaporation is known. Since, on the other hand, the main emphasis of this study was concerned with the significance of λ as the particle characteristic dimension and the validity of Equation (1), it was decided to report the experimental data in the form of graphs showing the amount of acetone evaporated (in milligrams) vs. λ for the particle, at a constant average air velocity and a constant air temperature (410°F.). Figure 4, 5, and 6 illustrate typical results at two different air velocities for spheres, cubes, and cylinders, respectively. The solid lines on each graph represent the total predicted evaporation calculated as follows:

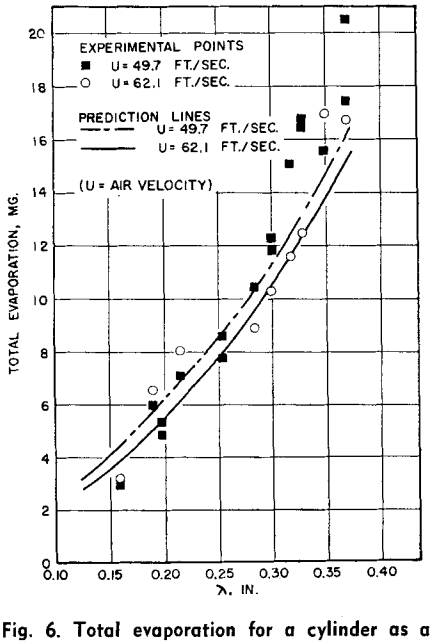

Fig. 6. Total evaporation for a cylinder as a function of its characteristic dimension.

A value of w (uncorrected for the effect of the high evaporation rate) was first calculated by means of Equation (1) integrated over the residence time of the particle in the apparatus, with the expression

$$w \text{ (in milligrams)} = \frac{(0.692)(1{,}000)(454)(M)(A)(\Delta_p)(G_m)}{(3{,}600)(P_{LM})(Sc)^{2/3}} \int_0^\theta \frac{d\theta}{(Re'')^{0.486}} \quad (13)$$

The diffusivity data for acetone evaporating in air at 410°F. (wet-

bulb temperature: 19.7°C.) were calculated from equations given by Fair and Lerner (*16*), yielding $(Sc)^{2/3} = 1.32$. The vapor pressure of acetone at 19.7°C. was taken as 183 mm. Hg. The integral in Equation (13) was estimated graphically, with the distance-time data illustrated in Figure 3.

To correct w, as calculated above, for the effect of the high evaporation rate resulting from the low latent heat of vaporization of acetone, a number of methods have been proposed (*5, 6, 17, 18*), none of which has however received extensive experimental verification. The Ranz correction, which was selected, may be summarized by

$$\frac{\text{Corrected evaporation}}{w} = \frac{\ln(1+B)}{B} \quad (14)$$

where

$$B = k_1 c_p \Delta t / k_{avg} \lambda_a = 0.308 \quad (15)$$

The following values were taken: $c_p = 0.38$(avg); $k_1 = 0.0107$; $k_{avg} = 0.0190$. Hence the corrected evaporation amounted to $0.87w$.

Discussion of Results

The typical experimental points shown in Figure 4, 5, and 6 follow the calculated prediction lines quite closely at small values of the diameter (for the spheres) or λ (for the cubes and cylinders) but deviate appreciably at larger values. As will be seen later the latter trend may be due to factors which are not accounted for by Equation (1), although the scatter obtained may be explained partially by the fact that the difference between two relatively large weights had to be taken to determine the initial acetone content, while the correction of 1.29% to account for the residual acetone left in the particle was not quite a constant value.

It is to be noted from the graphs that as the air velocity increases, the total acetone evaporated from a given particle in the column decreases. This behavior is similar to that observed in spray dryers (*8*) and in the Atomized Suspension Technique (*19*) and is due to the fact that, although the relative velocities encountered at a higher air velocity are increased and the evaporation rates therefore increased, the particle residence time is greatly reduced, causing an over-all reduction in evaporation. A comparison of Figure 5 with Figure 4 at an air velocity of 62.1 ft./sec. shows that for a given λ the evaporation from a cube in its flight through the column is greater than that from a sphere, owing to its greater surface, although its residence time is shorter (see Figure 3). The shape of the prediction curves for cylindrical particles in Figure 6 for the three diameters used, with different lengths, can be similarly accounted for from surface area and residence time considerations. When one considers the range studied, the agreement here is quite good.

CONCLUSIONS

The correlation of heat and mass transfer for nonspherical or irregular particles in terms of a suitable characteristic dimension or shape factor has always posed a serious problem in solids-gas systems. The various empirical approaches which have been proposed have seldom proven to be susceptible of generalization. In a previous study (*1*) it has been shown that the particle characteristic dimension was not only unusually successful in correlating existing data for stationary particles in various orientations but could also be justified qualitatively in terms of boundary-layer considerations, as long as only heat and mass transfer (skin friction) effects are involved. The latter fact is of some significance, since it removes for the first time some of the empiricity from the method of approach. The present work indicates that for randomly rotating particles λ (the average value of L'' over all possible orientations) probably represents the proper particle characteristic dimension; when used in the Reynolds number N_{Re}'' in conjunction with Equation (1) adequate prediction of the rates of heat and mass transfer were obtained, particularly at low values of λ.

It is interesting to note from Table 1 that for any prism or cylinder the values of λ and of the particle equivalent diameter D_p differ by no more than 3%. In other words within that small error the two parameters may be used interchangeably. This explains why D_p has sometimes been used successfully to correlate certain heat or mass transfer data in particulate systems involving a large number of randomly oriented particles, providing that only skin friction (rather than form drag) effects are considered. Thus in 1957 Bar-Ilan and Resnick (*20*), in a review of the published work on heat and mass transfer in packed beds, noted that for regularly shaped particles with diameters greater than 4 mm. the data could be correlated in the form of a single j_D (or j_H) vs. N_{Re} equation, with D_p as the characteristic dimension. The latter was obtained from experimental results and was completely empirical in nature. It is felt however that D_p has no theoretical significance as a characteristic dimension and its use cannot be justified in terms of the boundary-layer theory. Indeed it completely fails to correlate mass and heat transfer data for single particles.

At higher values of λ Equation (1) appears to give evaporation rates which are too low, due presumably to the presence of factors for which it does not account. When one assumes that the acceleration rate (130 ft./sec.^{2} approximately at the top of the column and about 35 ft./sec.^{2} at the bottom) has little effect on the rate of mass transfer, as indicated by the work of Manning (*8*), Ingebo (*7*), and Seban and Doughty (*2*), possible factors which may be responsible for the increased evaporation are fluid turbulence and particle rotation.

In 1956 Kays and Bjorklund (*3*) studied the effect of rotation on the rate of convective heat transfer to a cylinder rotating about its axis, the latter being fixed. Their empirical correlation indicates that such an effect is quite small unless the particle peripheral velocity reaches a magnitude comparable with that of the fluid relative velocity, which is not the case in the present study. It is doubtful whether this correlation would apply to freely moving particles.

The most plausible explanation for the higher rates of evaporation which were observed with the larger particles can probably be deduced from Torobin's work on momentum transfer (*13*). As already mentioned he has established that a laminar-turbulent transition will occur in the attached boundary layer of a freely moving sphere if, at a given value of the Reynolds number, the relative intensity of turbulence is high enough. Such transition will increase the rates of heat and mass transfer appreciably when it occurs (*21*). If the constant value of 45 found by Torobin in his wind-tunnel studies for the product (relative intensity of turbulence)^2 (initial particle N_{Re} at which transition occurs) is assumed to hold in the present investigation, it can be seen that transition cannot occur during the initial motion of the particles (irrespective of their size) because the relative intensity of turbulence (approximately 3% at the top) is much too small. As the particle accelerates down the column, its relative velocity decreases; the particle Reynolds number also decreases, but the relative turbulent intensity increases. Now it can be easily verified that for the smaller particles used under the conditions of the present investigation the critical product value of 45 was never attained, and no transition therefore occurred. Equation (1) applies quite well in this case, since it was

itself derived originally from experiments in which transition could not have taken place. For the larger particles however the critical product value of 45 was attained in the lower portion of the column, and transition very probably occurred, thus accounting for the higher rates of mass transfer.

These views concerning the effectiveness of a laminar-turbulent transition in the boundary layer, resulting from the relative intensity of turbulence, in increasing the rates of heat and mass transfer must at present remain qualitative. The experimental situation used in the present study was not specifically designed to provide the required quantitative data. Nor can this information be obtained from other published investigations of the effect of stream turbulence on heat and mass transfer, such as those of Loitsiansky and Schwab (*22*), Comings, Clapp, and Taylor (*23*), Haas van Dorser, Leniger, and van Meel (*24*) Maisel and Sherwood (*25*), and more recently those of Van der Hegge Zijnen (*26*) Schnautz (*4*) and Brown, Sato, and Sage (*27*). Most of these studies showed that an increase in intensity of turbulence was more effective in increasing the heat and mass transfer rates when the Reynolds number was high than when it was low (*4, 22, 23, 24, 25, 27*), a behavior which can be explained by the onset of transition under these conditions. The latter may also account for the marked increase in rates which occur at certain critical values of the Reynolds number and turbulence intensities (*25, 27*) which are compatible with those of the critical product mentioned previously; it may also explain the apparent lack of agreement between the results obtained by various authors working in different ranges of these two parameters (*23, 25, 27*).

Valid heat mass transfer information for particles in a turbulent fluid is unfortunately still limited, but the results from work now in progress will be extremely helpful for a fuller understanding of the effects of the free-stream vorticity on the boundary layer and wake flow, in which the ratio of the Eulerian scale of turbulence to the particle characteristic dimension may also play a part (*26*). In the meantime the approach proposed in this paper, based on the use of Equation (1) combined with the characteristic dimension λ, will provide a fair if somewhat conservative approximation of the mass and heat transfer rates. It should be emphasized however that the calculations require a knowledge of the particle residence time. From the present study and also from previous work (*8*) it is evident that an accurate estimation of the residence time cannot be obtained from the standard C_D vs. N_{Re} curve for Reynolds numbers greater than approximately unity. This region is of considerable practical importance in many contacting operations, such as the nozzle range of spray-dryers, cyclone evaporators, and Venturi scrubbers, in flash-drying, in conveying systems, and many others. The coefficient of drag is now known to be a complex function of the rate of acceleration of deceleration, of the turbulence characteristics of the fluid, as well as many other factors which affect the formation of the wake (particle shape and surface roughness, rate of vapor evolution, particle rotation, proximity to walls or other particles, etc.). Studies of some of these effects using the radioactive tracer technique are currently under way, and it is hoped that the results will permit more accurate predictions of the particle residence time.

ACKNOWLEDGMENT

Financial assistance from the National Research Council of Canada in the form of a research grant, and from Canadian Refractories Limited in the form of two fellowships awarded to I. S. Pasternak, is gratefully acknowledged. Recognition is also due to L. B. Torobin and L. Yaffe for their collaboration in the development of the velocity measuring technique, and to the Pulp and Paper Research Institute of Canada for the extensive use of their facilities.

NOTATION

$a,b,c,$ = sides of a prism, ft.
A = surface area of particle, sq. ft.
C_D = drag coefficient, dimensionless
c_p = specific heat at constant pressure, B.t.u./(lb.)(°F.)
D = diameter, ft.
d = diameter of cylinder, ft.
D_p = diameter of a sphere with same volume as particle, ft.
D_v = diffusion coefficient for acetone evaporating in air, sq. ft./sec.
g = gravitational constant = 32.2 ft./sec.^{2}
G = mass velocity of flowing air, lb./(sq. ft.)(sec.)
G_m = molal mass velocity of flowing air, lb. moles/(sq. ft.)(hr.)
h = heat transfer coefficient, B.t.u./(hr.)(sq. ft.)(°F.)
k_f = average thermal conductivity of air film, B.t.u./(hr.)(ft.)(°F.)
k_g = mass transfer coefficient, lb. moles/(hr.)(sq. ft.)(Δp)
k_1 = thermal conductivity of air and acetone vapors at acetone wet-bulb temperature, B.t.u./(hr.)(sq. ft.)(°F.)
k_{avg} = average thermal conductivity of air in transfer region, B.t.u./(hr.)(ft.)(°F.)
L = length, ft.
L'' = characteristic dimension for stationary particle, ft.
M = molecular weight of acetone, lb./lb. mole
P_{LM} = log mean pressure difference of air across the boundary layer, atm.
Δp = driving force, atm.
s = distance down column, ft.
Δt = temperature difference across air-acetone boundary layer, °F.
U = average air velocity, ft./sec.
v = volume of particle, cu. ft.
V_p = cylinder surface peripheral velocity, ft./sec.
V_r = velocity of particle relative to the air stream, ft./sec.
w = mass of acetone evaporated, mg.

Greek Letters

α,β,γ = angles of rotation, deg.
β' = coefficient of volume expansion of vapor film, 1/°F.
θ = time, sec.
λ = characteristic dimension for freely rotating particle, ft.
λ_a = latent heat of vaporization of acetone, B.t.u./lb.
μ_f = average viscosity of air film, lb. mass/(ft.)(sec.)
ρ_f = average density of air film, lb. mass/(ft.)^3

Dimensionless Groups

$B = k_1 c_p (\Delta t)/k_{avg}\lambda_a$
N_{Gr} = Grashof Number = $D^3\rho_f^2 g\beta'\Delta t/\mu_f^2$
j_D = mass transfer factor = $(k_G P_{LM}/G_m)(Sc)^{2/3}$
N_{Nu} = Nusselt number for heat transfer = hD/k_f
$N_{Nu'}$ = modified Nusselt number for mass transfer = $k_G L''RT/D_v$ or $k_G\lambda RT/D_v$
N_{Pr} = Prandtl number for heat transfer = $c_p\mu_f/k_f$
N_{Re} = normal flow Reynolds number = DG/μ_f
N_{Re}'' = $L''G/\mu_f$ or $\lambda V_r\rho_f/\mu_f$
N_{Re_r} = $DV_p\rho_f/\mu_f$
N_{Sc} = Schmidt number for mass transfer = $\mu_f/D_v\rho_f$

LITERATURE CITED

1. Pasternak, I. S., and W. H. Gauvin, *Can. J. Chem. Eng.*, 38, 35 (April, 1960).
2. Seban, R. A., and D. L. Doughty, *Trans. Am. Soc. Mech. Engrs.*, 78, 217 (1956).

3. Kays, W. M., and I. S. Bjorklund, *Tech. Rept. 30*, Stanford Univ., Stanford, California (1956).
4. Schnautz, J. A., Ph.D. thesis, Oregon State College, Corvallis (1958).
5. Marshall, W. R., *Chem. in Canada*, **7**, 37 (1955).
6. Ranz, W. E., *Trans. Am. Soc. Mech. Engrs.*, **78**, 909 (1956).
7. Ingebo, R. D., *Natl. Advisory Comm. Aeronaut., Tech. Note 3762* (1956).
8. Manning, W. P., and W. H. Gauvin, *A.I.Ch.E. Journal*, **6**, 184 (1960).
9. Kolthoff, I. M., and R. Belcher, "Volumetric Analysis," Vol. 3, p. 380, Interscience, New York (1957).
10. Sutton, F., and J. Grant, "A Systematic Handbook of Volumetric Analysis," 13 ed., p. 482, Butterworths Scientific Publication, London (1955).
11. Gauvin, W. H., I. S. Pasternak, L. B. Torobin, and L. Yaffe, *Can. J. Chem. Eng.*, **37**, No. 3, 95 (1959).
12. Lapple, C. E., and C. B. Shepherd, *Ind. Eng. Chem.*, **32**, 605 (1940).
13. Torobin, L. B., and W. H. Gauvin, *Can. J. Chem. Eng.*, **38**, 24 (1960);
13a. ———, *A.I.Ch.E. Journal*, to be published.
14. Sandborn, B. A., *Natl. Advisory Comm. Aeronaut., Tech. Note 3266* (1955).
15. Gauvin, W. H., and S. G. Mason, *Chem. Engr. Progr.*, **55**, No. 6, 49 (1959).
16. Fair, J. R., and B. J. Lerner, *A.I.Ch.E. Journal*, **2**, 13 (1956).
17. Godsave, G. A. E., "Collected Papers of the 4th Int. Symp. on Combustion," Cambridge, Mass. (Sept., 1952).
18. Spalding, D. B., *Proc. Roy. Soc. (London)*, **A221**, 78 (1954).
19. Gauvin, W. H., *Tappi*, **40**, No. 11, 866 (1957).
20. Bar-Ilan, M., and W. Resnick, *Ind. Eng. Chem.*, **49**, 313 (1957).
21. Edwards, A., and B. N. Furber, *Proc. Inst. Mech. Engrs.*, **170**, 941 (1956).
22. Loitsiansky, L. G., and B. A. Schwab, *Central Aerod. Hydr. Inst. Moscow, Rept. No. 329* (1935).
23. Comings, E. W., J. T. Clapp, and J. F. Taylor, *Ind. Eng. Chem.*, **40**, 1076 (1948).
24. Haas van Dorsser, A. M., H. A. Leniger, and D. A. Meel, *Chem. Ing.*, **25**, 61 (1949).
25. Maisel, D. S., and T. K. Sherwood, *Chem. Eng. Progr.*, **46**, 172 (1950).
26. Van der Hegge Zijnen, B. G., *Appl. Sci. Research*, **A7**, 205 (1958).
27. Brown, R. A. S., K. Sato, and B. H. Sage, *Ind. Eng. Chem., Data Series*, **3**, 263 (1958).

Manuscript received September 28, 1959; revision received October 3, 1960; paper accepted October 5, 1960. Paper persented at A.I.Ch.E. San Francisco meeting.

The Mechanics of Moving Vertical Fluidized Systems: V. Concurrent Cogravity Flow

J. A. QUINN, LEON LAPIDUS, and J. C. ELGIN

Princeton University, Princeton, New Jersey

An experimental investigation of the concurrent cogravity flow of particulate solids and water in a 1-in. diameter vertical column is reported. Measurements were made of the particle concentration, or holdup, existing in the column as a function of the fluid and particle flow rates for two particle sizes, 0.0184- and 0.00396-in. diameter glass spheres. The experimental results form the basis for a prediction of the generalized characteristics of concurrent cogravity fluidization.

The data for each particle size are correlated in terms of the slip velocity and the holdup. The slip velocity is demonstrated to be the same unique function of the holdup for concurrent cogravity flow and for batch fluidization. Therefore the holdup and the conditions of limiting operation for concurrent cogravity flow can be accurately predicted from the batch fluidization curve.

This publication represents the fifth in a series of investigations of the mechanics of moving fluidized systems. Previous publications (*1, 2, 3, 4*) have discussed a generalized theory of vertical fluidized systems and the experimental validation of this theory as applied to countercurrent and concurrent countergravity flow. As a consequence of this theoretical analysis a relatively new technique for fluid-particle contacting was recognized. The operating characteristics predicted for this type of flow, concurrent cogravity, indicated some rather unique possibilities of contacting, and this investigation was undertaken to study the behavior of such fluid-particle systems.

The theoretical background developed in this program has been detailed by Elgin and Lapidus (*1*), and the salient aspects will be outlined here. Of fundamental importance is the slip velocity defined as the difference between the net fluid and particle velocities. To suitably define this term the convention is adopted that upward flow in a vertical system is positive. It is assumed that the slip velocity is a unique function of the holdup in any fluidized system and thus independent of the relative direction of flow of fluid and particles with respect to each other. The holdup is equal to the volume of particles per unit volume of particles plus fluid.

The relationship between the slip velocity and the holdup can be readily obtained for a fluid-solid system from a batch-fluidization experiment where the net particle velocity is zero and the slip velocity is equal to the average fluid velocity in the bed. The holdup per unit volume is inversely proportional to the expanded bed height; therefore by determining the expanded bed height as a function of the rate of fluid flow into the bed an empirical relation between the slip velocity and the holdup can be obtained for any particular system..

If the slip velocity is a unique function of holdup, the operating characteristics of the various types of vertical fluidized systems can be predicted quantitatively from the results of a single batch fluidization experiment or from one of the generalized correlations which have been published for batch-fluidization data (*5, 6*).

Earlier work in this program has substantiated the predictions concerning the behavior of free countercurrent and free concurrent countergravity flow. Price (*2*) studied three different particle sizes in free countercurrent flow and obtained data in close agreement with predictions from batch-fluidization results. Struve (*3*) investigated concurrent countergravity flow and also substantiated the predicted relation of holdup to slip velocity. Hoffman (*4*) extended the principles to cover the case of mixed-size particles.

At the present time the literature shows only two references to free concurrent cogravity flow. Price (*2*), in the course of his work on countercurrent flow, made one determination of holdup in concurrent cogravity flow. This experiment was performed to demonstrate that higher holdups could be obtained in concurrent cogravity

J. A. Quinn is at the University of Illinois, Urbana, Ill.